DOI: 10.1021/jm901877j

Journal of Medicinal Chemistry Article

Synthesis and Biological Evaluation of 4-Anilinoquinolines as Potent Inhibitors of Epidermal Growth Factor Receptor

Vijaykumar G. Pawar,[†] Martin L. Sos,[‡] Haridas B. Rode,[†] Matthias Rabiller,[†] Stefanie Heynck,[‡] Willem A. L. van Otterlo,[†,∥] Roman K. Thomas,[†,‡,§] and Daniel Rauh*[,†]

[†]*Chemical Genomics Centre of the Max Planck Society, Otto-Hahn-Strasse 15, 44227 Dortmund, Germany,* [‡]*Max Planck Institute for Neurological Research with Klaus-Joachim-Zülch Laboratories of the Max Planck Society and the Medical Faculty of the University of Köln, Gleueler Strasse 50, 50931 Köln, Germany,* [§]*Department I of Internal Medicine and Center of Integrated Oncology Köln—Bonn, University of Köln, 50924 Köln, Germany, and* [∥]*Molecular Sciences Institute, School of Chemistry, University of the Witwatersrand, Johannesburg, South Africa*

Received December 20, 2009

The mutant receptor tyrosine kinase EGFR is a validated and therapeutically amenable target for genotypically selected lung cancer patients. Here we present the synthesis and biological evaluation of a series of 6- and 7-substituted 4-anilinoquinolines as potent type I inhibitors of clinically relevant mutant variants of EGFR. Quinolines **3a** and **3e** were found to be highly active kinase inhibitors in biochemical assays and were further investigated for their biological effect on EGFR-dependent Ba/F3 cells and non-small cell lung cancer (NSCLC) cell lines.

Introduction

The tyrosine kinase epidermal growth factor receptor (EGFR[a]) and its closely related family member HER2 are recognized targets for targeted cancer therapy and have been extensively investigated by both academia and industry.[1] Since the 1980s, when EGFR and HER2 were proposed as potential anticancer targets, small molecule kinase inhibitors and monoclonal antibodies have emerged as promising strategies to inhibit EGFR and HER2 kinase activity.[2] To date, the Food and Drug Administration has approved 11 small molecule kinase inhibitors for targeted cancer therapy[3] and dozens are currently in clinical trials. Out of these 11 inhibitors, Gefitinib, Erlotinib, and Lapatinib (Figure 1) belong to a class of 4-anilinoquinazolines which have been designed to target the ATP binding pocket of the kinase domain and are approved for the treatment of EGFR/HER2-dependent tumors which occur in non-small cell lung cancer (NSCLC) or breast cancer.[4] Although a plethora of quinazoline-based kinase inhibitors are known and widely used in medicinal chemistry and chemical biology research, examples of type I kinase inhibitors based on the closely related quinoline scaffold are few in number.

Type I inhibitors are ATP competitive and bind to the hinge region of the enzymatically active kinase domain and represent the prototypical kinase inhibitor. One of the first extensive SAR studies on type I inhibitors active on EGFR was published in 1995 by researchers at Parke-Davis[5] in which Rewcastle and colleagues reported a SAR study on a series of compounds derived from ten-membered nitrogen-containing bicyclic scaffolds. They concluded that the quinazoline core was the best scaffold for the development of EGFR inhibitors because any alteration of the nitrogen substitution pattern in the bicyclic ring resulted in less active compounds.[5] In particular, the replacement of the N3 of the quinazoline **1** by a CH resulted in a 200-fold drop in affinity (Figure 1). At the same time, based on modeling studies, scientists at Wyeth[6] hypothesized that the quinazoline N3 interacts with the kinase domain via a water-mediated hydrogen bond to the side chain of the gatekeeper Thr790 of EGFR and provided a rationalization for the crucial role of N3 of the quinazoline core for activity (Figure 2a). On the basis of these findings, Wissner et al.[7] developed a series of compounds where the N3 of the quinazoline was replaced by a C−CN group to: (a) displace the hypothetical water molecule and (b) to serve as a hydrogen bond acceptor for the Thr790 hydroxyl group (Figure 2b,c). Through this elegant application of a bioisostere, Wissner and colleagues were not only able to generate potent inhibitors of EGFR (e.g. Neratinib, currently in clinical trials) but also to resolve overlapping patent applications with Parke-Davis. This binding mode of quinazolines to the hinge region of the kinase domain and the interaction of N3 with the side chain of the gatekeeper Thr790 via a water molecule was coined in 2002 when researchers at Genentech published the crystal structure of EGFR in complex with Erlotinib (PDB code: 1M17)[8] and has since then served as an important reference for the structure-based design of both reversible and irreversible EGFR and HER2 kinase inhibitors.[7,9−11]

In our studies of the inhibition of EGFR and clinically relevant drug resistant mutant variants by reversible and irreversible 4-anilinoquinazolines,[12] we could not correlate the importance of the discussed water-mediated hydrogen bond with potent inhibition of EGFR. This stimulated our interest in designing and synthesizing of a series of 6,7-substituted 4-anilinoquinolines to compare SAR with their

*To whom correspondence should be addressed. Phone: +49 (0)231-9742 6480. Fax: +49 (0)231-9742 6479. E-mail: daniel.rauh@cgc.mpg.de.

[a]Abbreviations: EGFR, epidermal growth factor receptor; TKIs, tyrosine kinase inhibitors; HTRF, homogeneous time-resolved fluorescence; NSCLC, non-small cell lung cancer; GI_{50}, concentration at which 50% growth retardation is observed.

 Published on Web 03/11/2010

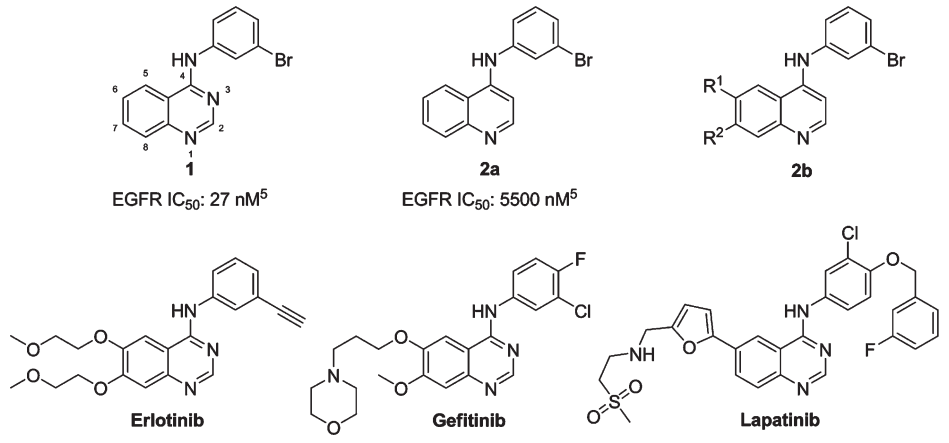

Figure 1. Structures of 4-anilinoquinazoline- and 4-anilinoquinoline-based EGFR/HER2 inhibitors. Simple 4-anilinoquinazolines such as **1** served as starting points for the development of potent type I and type II EGFR/HER2 inhibitors approved for the treatment of NSCLC. Erlotinib and Gefitinib are type I inhibitors and bind to the ATP site of activated kinases. Lapatinib is a type II inhibitor and stabilizes enzymatically inactive kinase conformations of EGFR and HER2. According to earlier studies, quinolines such as **2a** show reduced activity against EGFR and are less suited for compound optimization.[5] **2b** represents a series of 6- and 7- substituted 4-anilinoquinolines as potent type I inhibitors of clinically relevant mutant variants of EGFR discussed in this study.

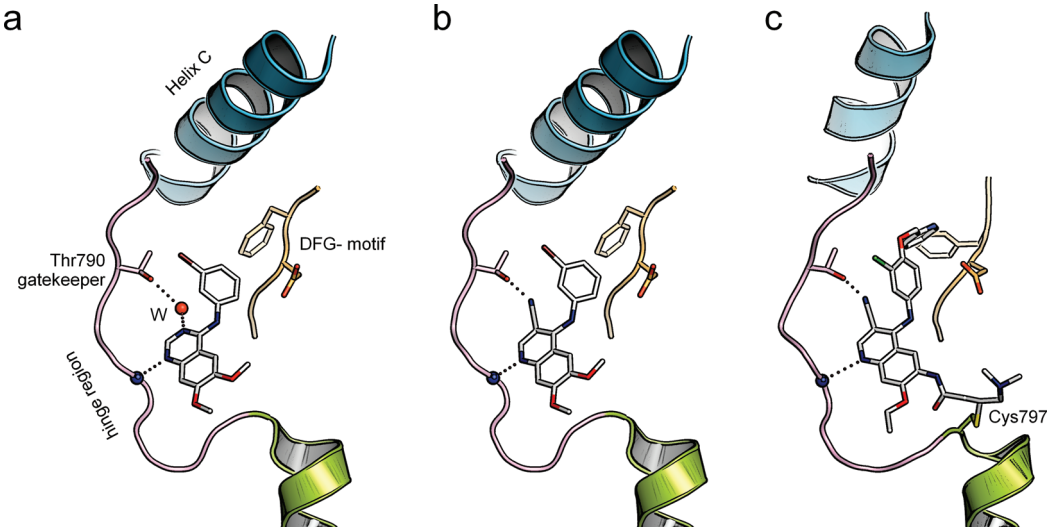

Figure 2. Binding modes of 4-anilinoquinazoline- and 4-anilinoisoquinoline-based EGFR and HER2 inhibitors. (a) Proposed binding mode of a 4-anilinoquinazoline to the ATP-binding site of EGFR. Hydrogen bonding interactions of the inhibitor with the hinge region (pink) and the side chain of the gatekeeper residue Thr790 (mediated via a water molecule (W)) are shown as red dotted lines. (b) This binding mode stimulated the design and synthesis of 3-quinolinecarbonitriles to displace the proposed water molecule and to form a direct hydrogen bond to the side chain of gatekeeper residue (Thr790).[7] (c) The presence of a less conserved Cys at the lip of the ATP pocket fostered the development of irreversible quinazoline and isoquinoline EGFR inhibitors currently in clinical trials. The irreversible inhibitor Neratinib is modeled to the catalytic domain of EGFR. Modeling is based on the crystal structure of Neratinib in complex with drug resistant EGFR-Thr790Met (PDB code: 2JIV).[15] The electrophile of the inhibitor forms a covalent bond with the side chain of Cys797. Cys797 is located at the N-terminal end of a short helix and activated by the helix dipole. Both reversible and irreversible 3-quinolinecarbonitriles were designed to (a) displace the water molecule (W10), and (b) to form a direct hydrogen bond to the side chain hydroxyl of the gatekeeper Thr790.[7]

direct quinazoline-based homologues and to investigate their inhibition of EGFR and its clinically relevant mutant variants, both in biochemical and in cellular assays.

Results and Discussion

The design and synthesis of the quinoline inhibitors evolved from our previous studies aimed to address questions of how to overcome Thr790Met drug resistance in EGFR using small organic molecules.[12] One of the key challenges in targeted cancer therapy is the emergence of drug resistance mutations in the primary target. At the gatekeeper position, mutations leading to sterically demanding amino acids have been observed in BCR/ABL (Thr315Ile), c-KIT (Thr670Ile), the platelet-derived growth factor receptor-α (PDGFRα, Thr674Ile), and EGFR (Thr790Met). All of them result in tumor drug resistance.[13,14] In wild type kinases, the gatekeeper residue is a smaller amino acid located in the hinge region of the kinase domain and controls access to the hydrophobic subpocket, thereby playing a crucial role in inhibitor affinity and selectivity (Figure 2).[2] It has also been shown that these mutations prevent binding of kinase inhibitors such as Imatinib, Gefitinib, and Erlotinib due to steric hindrance and/or an increase in ATP affinity,[15] highlighting the necessity for the development of novel strategies to design inhibitors capable of overcoming mutation-associated drug resistance in kinases.[16] Our previous structural and functional

Table 1. Focused Library of Designed 4-Anilinoquinoline-Based Inhibitors and their 4-Anilinoquinazoline Counterparts[a]

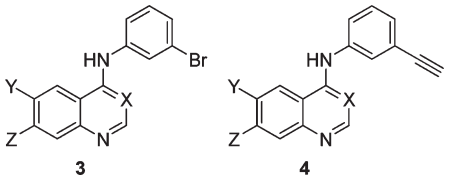

Compd	X	Y	Z	IC_{50} in nM		
				EGFR-WT	EGFR-Leu858Arg	EGFR-Leu858Arg, Thr790Met
3a	CH	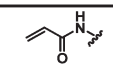	H	< 1 nM	< 1 nM	3.2 ±1.6
3b	N	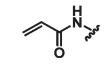	H	<1 nM	1.1 ±0.8	< 1 nM
3c	CH	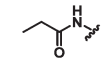	H	16 ±6	2.8 ±2.6	520 ±280
3d	N	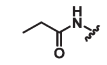	H	0.1 ±0.04	0.4 ±0.6	1000 ±1300
3e	CH	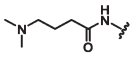	H	1.7 ±0.5	0.5 ±0.07	130 ±16
3f	N	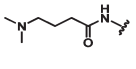	H	<1 nM	<1 nM	190 ±69
4a	CH	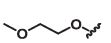	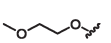	30 ±9	14 ±4	1500 ±150
Erlotinib	N	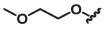	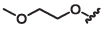	0.2 ±0.05	0.1 ±0.05	1000 ±360
4b	CH	-OMe	-OMe	19 ±11	4 ±2	1500 ±670
4c	N	-OMe	-OMe	<1 nM	<1 nM	140 ±24

[a] The structures of reversible and irreversible 4-anilinoquinoline- and 4-anilinoquinazoline-based inhibitors are shown. On the basis of their binding mode to the kinase domain of EGFR, the individual inhibitors are classified as follows: irreversible **3a**; reversible **3c**, **3e**, and **4a**,**b**, quinolines and irreversible **3b**; reversible **3d**, **3f**, Erlotinib and **4c**, quinazolines. IC_{50} values were measured with an activity based phosphorylation assay (HTRF). Both reversible and irreversible quinolines give IC_{50} values more or less comparable to their quinazoline counterparts, demonstrating that the 4-anilinoquinoline-core is indeed suitable for targeting EGFR.

studies alluded toward the possibility of a steric clash between the Met gatekeeper in drug resistant EGFR-Thr790Met and the 3-bromoanilino moiety at the 4-position of quinazoline inhibitors.[12,17] We reasoned that the binding of ligands such as erlotinib to EGFR-Thr790Met would not only be hampered by this steric hindrance but also due to the loss of the water-mediated hydrogen bond to the side chain hydroxyl of the Thr790 of EGFR-WT, an interaction which is not possible with the side chain of the mutated Met790. However, we were puzzled by the fact that although EGFR-Thr790Met is a drug resistant mutation with fatal outcome in affected patients, reversible quinazolines such as Erlotinib and Gefitinib lose potency by only 2−3 orders of magnitude while irreversible 4-anilinoquinazolines still inhibit EGFR-Thr790Met in the subnanomolar range in biochemical assays.[12,17] We hypothesized that if the N3 of the quinazoline does play an essential role in binding to EGFR, via the formation of a hydrogen bond, the gatekeeper Thr to Met mutation should have resulted in a much more dramatic loss of activity. Therefore, we investigated the requirement of a nitrogen atom at the 3-position of the ten-membered ring system (e.g., **2a**, Figure 1) for potent inhibition of EGFR and proposed, contrary to the SAR reported by Rewcastle et al.,[5] that 6,7-substituted quinolines (**2b**, Figure 1) would also be effective inhibitors of EGFR. Excluding the direct steric effect of the Met790 side chain on binding, we believed that the binding mode of the quinoline inhibitor (**2b**, Figure 1) to EGFR-WT would be comparable to that of an analogous quinazoline-based

Scheme 1. Synthesis of Quinoline and Quinazoline Derivatives I[a]

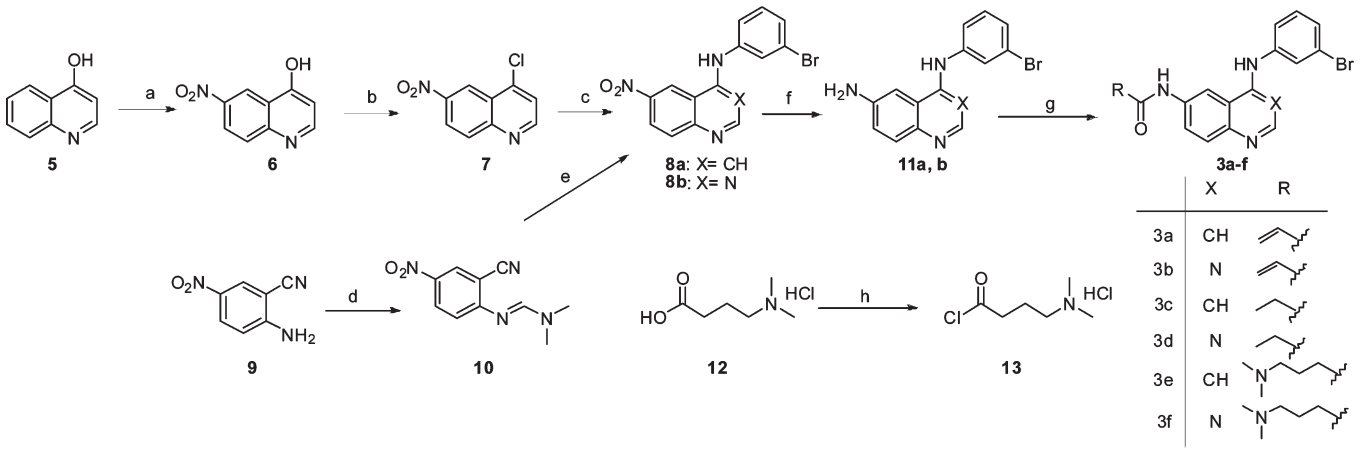

[a] Reagents and conditions: (a) HNO_3/H_2SO_4, −15 to 0 °C; (b) $POCl_3$, cat. DMF, reflux; (c) 3-bromoaniline, cat. conc HCl, isopropyl alcohol, reflux; (d) DMF acetal, reflux; (e) 3-bromoaniline, HOAc, reflux; (f) Fe, HOAc, aq EtOH, reflux; (g) RCOCl, DIEA, THF, 0 °C to rt; (h) oxalyl chloride, CH_2Cl_2, cat. DMF, reflux, 30 min. Compound **3f** was synthesized from **11b** and 4-(dimethylamino)butyric acid hydrochloride **12**, EDCI.HCl, triethylamine, DMF, 0 °C to rt, overnight.

Scheme 2. Synthesis of Quinoline and Quinazoline Derivatives II[a]

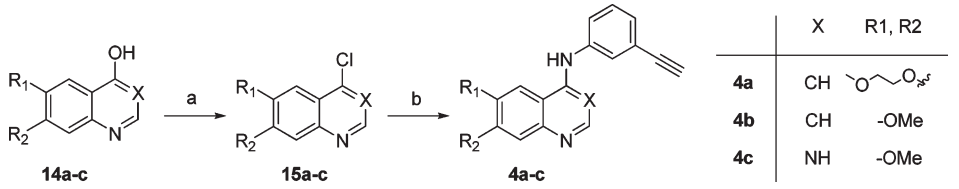

[a] Reagents and conditions: (a) $POCl_3$, cat. DMF, reflux; (b) 3-ethynylphenylamine, cat. conc HCl, isopropyl alcohol, reflux.

inhibitor bound to drug resistant EGFR-Thr790Met because hydrogen bonding with a Thr790 is not possible in either situation. However, taking these direct steric effects into consideration, the potency of the 4-anilinoquinoline inhibitors against EGFR-WT would be expected to be better than the potency of the more traditional quinazoline-based inhibitors like Erlotinib against EGFR-Thr790Met.

Interestingly, at the time we were synthesizing a series of 4-anilinoquinolines to test our hypotheses, the structure factors of the EGFR−Erlotinib complex were made available to the public (PDB code: 1M17).[8] This allowed us to calculate the corresponding electron density maps (Supporting Information Figure 1), and we were surprised to find that there was no electron density supporting the existence of a water molecule mediating the binding of N3 of the quinazoline core to the side chain of Thr790, further stimulating our design of quinoline-based type I kinase inhibitors. To explore the SAR, based on our prediction that the N3 of the quinazoline core should not play a central role in binding to EGFR, we synthesized different quinoline and quinazoline inhibitors and screened these against EGFR and its mutant variants (Leu858Arg and Leu858Arg-Thr790Met) in biochemical (Table 1) and cellular assays (Figure 4), respectively.

Chemistry. Quinoline and quinazoline inhibitors (**3a**−**f** and **4a**−**c**, Table 1) were designed to perform comparative SAR studies. 4-Anilinoquinolines **3a**,**c**,**e** (Table 1) and 4-anilinoquinazolines **3b**,**d**,**f** (Table 1) were synthesized starting from the intermediates **8a** and **8b**, respectively. These intermediates were synthesized by two different routes as described in Scheme 1. Synthesis of **8a** was achieved by regioselective nitration of 4-hydroxyquinoline **5** at the 6-position, using nitric acid in sulfuric acid at −15 °C, to afford

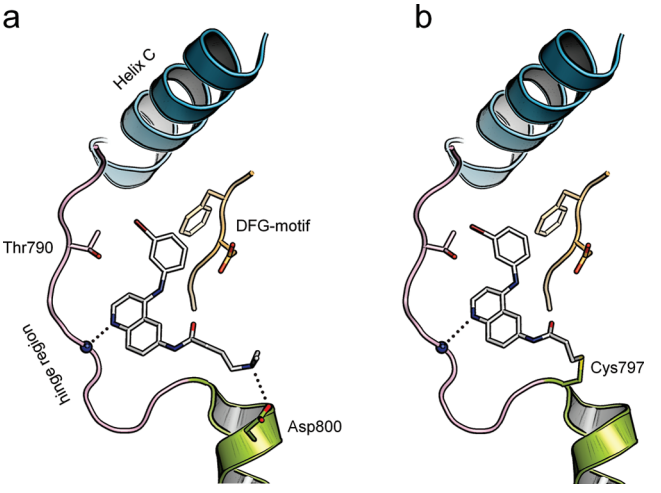

Figure 3. Proposed binding mode of 4-anilinoquinolines to EGFR. (a) **3e** is modeled into the ATP-binding site of EGFR based on the crystal structure of Erlotinib in complex with EGFR (PDB code: 1M17) and an irreversible quinazoline in complex with cSrc (PDB code: 2QLQ). The ring nitrogen of the quinoline forms a hydrogen bond (red dotted line) with the backbone of the hinge region (pink). The protonated tertiary amine of **3e** is within hydrogen bonding distance to the side chain of Asp800. This additional interaction is not observed for different substituted quinolines and helps to explain the gain in affinity for **3e**. (b) The irreversible 4-anilinoquinoline **3a** is modeled into the ATP-binding site of EGFR based on the crystal structure of its quinazoline counterpart to EGFR (PDB code: 2J5F).[26] The electrophile of the inhibitor forms a covalent bond to the side chain of Cys797.

6-nitro-4-hydroxyquinoline **6**. Chlorination of **6** resulted in the 4-chloro-6-nitroquinoline **7**, which was heated at reflux

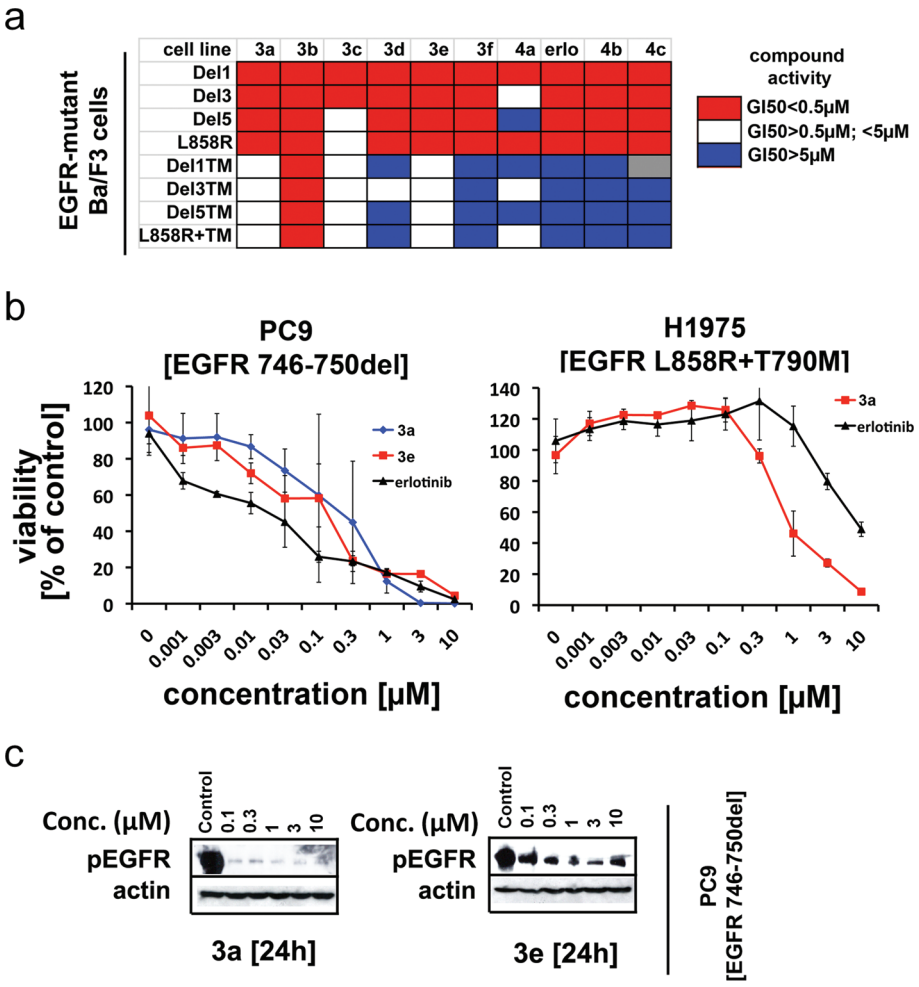

Figure 4. 4-Anilinoquinolines inhibit growth of EGFR-dependent cancer cells. (a) GI_{50} values for 4-anilinoquinoline- and 4-anilinoquinazoline-based EGFR inhibitors screened against Ba/F3 cell lines expressing different EGFR mutants with or without the secondary Thr790Met gatekeeper mutation (TM). The range of compound activity is color-coded. (b) The EGFR mutant NSCLC cell line PC9 was treated with increasing concentrations of **3a** (irreversible) and **3e** (reversible), and cell viability was determined using measurement of ATP content. The error bars represent the standard deviation for three replicates. (c) The NSCLC cell line H1975 expressing the Thr790Met EGFR gatekeeper mutation was treated with increasing concentrations of **3a** and **3e**, and cell viability was determined using measurement of ATP content. The error bars represent the standard deviation for three replicates. (d) Inhibition of the activation status of EGFR was determined by immunoblotting after treatment of PC9 cells with increasing concentrations of **3a** and **3e** (from left to right: control, 0.1, 0.3, 1, 3, 10 μM); actin was detected as loading control.

with 4-bromoaniline and catalytic amounts of hydrochloric acid in isopropyl alcohol to give **8a**. The intermediate **8b**, which was required for the synthesis of quinazolines **3b**, **3d**, and **3f**, was obtained by starting from 2-amino-5-nitrobenzonitrile **9**, which on treatment with dimethylformamide−dimethylacetal (DMF−DMA) in toluene produced the *N*,*N*-dimethylformamidine derivative **10** (Scheme 1). Compound **10** was heated at reflux with 3-bromoaniline in acetic acid to give intermediate **8b**. Finally, the nitro groups of **8a**,**b** were reduced using iron in acetic acid, followed by acylation of the resulting amines **11a**,**b** with the corresponding acid chlorides to obtain the 4-anilinoquinoline and quinazoline derivatives **3a**−**e** (Scheme 1). 4-(Dimethylamino)butanoyl chloride **13** required for **3e** was synthesized in situ from the corresponding acid **12** using oxalyl chloride and catalytic amounts of DMF. Compound **3f** was synthesized from **11b** and 4-(dimethylamino)butyric acid hydrochloride **12**, using 1-ethyl-3-(3-dimethylaminopropyl) carbodiimide hydrochloride (EDCI·HCl) as a coupling reagent. The 4-hydroxyquinoline and quinazoline derivatives **14a**−**c**, required for the synthesis of the 6,7-disubstituted 4-anilinoquinolines and quinazolines **4a**−**c**, were prepared by using procedures described in the literature.[17−19] The 4-hydroxyquinoline and quinazoline derivatives **14a**−**c** were subsequently treated with phosphorus oxychloride and catalytic *N*,*N*′-dimethylformamide to afford **15a**−**c**. Finally, **4a**−**c** were obtained from **15a**−**c** by the treatment with commercially available 3-ethynylphenylamine and a catalytic amount of concentrated hydrochloric acid in isopropyl alcohol (Scheme 2).

Biochemical Screening. To test the above-mentioned hypotheses regarding inhibition of EGFR by 4-anilinoquinolines, enzyme activity assays were performed for EGFR wild type and the two clinically relevant mutant variants EGFR-Leu858Arg (inhibitor-sensitizing mutation) and EGFR-Leu858Arg-Thr790Met (drug resistant mutation), respectively (Table 1). Although potencies of the inhibitors varied between the tested mutant kinases, the measured IC_{50} values showed the expected trends for reversible and irreversible inhibitors. We observed that all reversible and irreversible 4-anilinoquinoline-based inhibitors showed low to subnanomolar IC_{50} values on EGFR wild type and EGFR-Leu858Arg. When compared to their reversible quinazoline

	Gatekeeper	3e	3f
HER4	Thr	-10	-12
Lck	Thr	1	3
YES1	Thr	4	7
EPH-B3	Thr	5	17
RIPK2	Thr	10	10
MINK1	Met	12	35
Src	Thr	13	44
PKD1	Met	14	18
MNK2	Phe	21	14
MELK	Leu	25	49
PHK	Phe	26	10
EPH A2	Thr	26	53
CHK2	Leu	27	38
GCK	Met	30	48
CAMK1	Met	30	57
p38a	Thr	30	63
FGF-R1	Val	31	37
DYRK3	Phe	32	27
Aurora B	Leu	33	21
BRSK2	Leu	36	29
PRK2	Met	36	37
VEG-FR	Val	36	50
BTK	Thr	36	79
NUAK1	Met	37	39
CK1	Met	44	66
MKK1	Met	45	29
PIM1	Leu	46	12
BRSK1	Leu	46	52
SmMLCK	Leu	48	18
JNK1	Met	49	76
JNK2	Met	50	77
DYRK2	Phe	52	51
SYK	Met	57	67
PKBb	Met	61	80
JNK3	Met	62	72
IKKb	Met	62	90
p38b	Thr	63	81
MetNK1	Phe	64	49
PIM3	Leu	66	32
PAK5	Met	68	84
IRAK4	Tyr	70	81
IGF-1R	Met	71	105
MAPKAP-K3	Met	72	81
CSK	Thr	73	63
CAMKKb	Phe	74	66
RSK2	Leu	74	78
PIM2	Leu	75	62
MARK4	Met	75	74

	Gatekeeper	3e	3f
SRPK1	Phe	75	87
p38d	Met	76	79
MARK2	Met	77	82
PDK1	Leu	78	88
IRR	Met	79	70
PAK2	Met	79	75
PAK4	Met	79	83
MLK1	Met	79	87
MST4	Met	80	88
MST2	Met	80	90
PKCa	Met	81	78
SGK1	Leu	82	72
ERK1	Gln	82	83
PAK6	Met	82	93
AMPK	Met	83	70
CHK1	Leu	83	79
MLK3	Met	84	65
TBK1	Met	84	75
PRAK	Met	84	89
DYRK1A	Phe	85	65
NEK6	Leu	85	77
ERK8	Phe	85	78
IR-HIS	Met	85	79
TTK	Met	85	86
PKCz	Ile	86	86
MAPKAP-K2	Met	86	90
PKA	Met	86	91
S6K1	Leu	87	75
Aurora A	Leu	88	66
ERK2	Gln	88	88
CDK2-CycA	Phe	88	93
ROCK 2	Met	88	95
RSK1	Leu	89	72
GSK3b	Leu	89	96
CK2	Phe	90	96
IKKe	Met	92	89
p38g	Met	94	85
MARK3	Met	94	86
LKB1	Met	94	103
NEK2a	Met	95	96
MSK1	Leu	96	93
HIPK3	Phe	96	106
EF2K	Met	99	91
PKBa	Met	100	103
HIPK1	Phe	103	126
HIPK2	Phe	104	97
PLK1	Leu	109	95

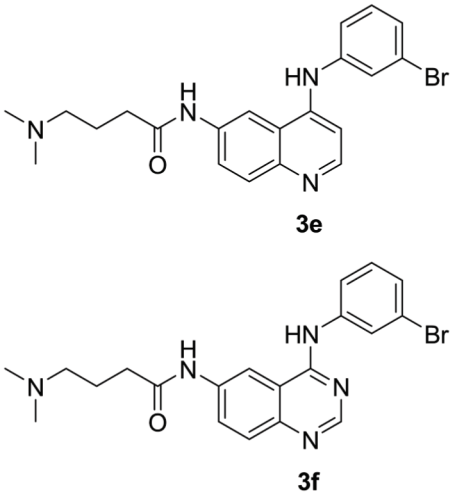

Figure 5. Kinase selectivity profile of **3e** and **3f**. Kinase profiling was performed for **3e** and **3f** against a panel of 95 different protein kinases at a concentration of 10 μM (National Centre for Protein Kinase Profiling, University of Dundee, UK). The screening was carried out using a radioactive (^{33}P-ATP) filter-binding assay. The scores represent the % activity remaining relative to the 100% DMSO controls. The inhibition is color coded from red (strong inhibition, low score) to green (weak inhibition, high score). Both quinazoline- and quinoline-based inhibitors show preference for kinases with a small amino acid at the gatekeeper position (Thr).

counterparts, quinolines **3c**, **4a** (corresponding quinoline to the marketed drug Erlotinib), and **4b** showed decreased potency by 1−2 orders of magnitude. Interestingly, this trend was not observed for **3e**, a quinoline containing an *N*,*N*-dimethylamino-butynoyl group in the 6-position of the quinoline core. The design of this compound and its quinazoline counterpart **3f** was stimulated by a charged interaction we previously observed for irreversible quinazoline-based EGFR inhibitors, decorated with an (*E*)-4-(dimethylamino)-but-2-enamide electrophile in the quinoline 6-position, bound to mutant variants of the tyrosine kinase cSrc (PDB codes: 2QQ7 and 2QLQ).[12] In these structures, the *N*,*N*-dimethylamino group is within hydrogen bonding distance to the side chain of Asp348. cSrc and EGFR share high identity in sequence (37% overall) and structure and the ATP binding sites are highly conserved (70%). Structural modeling of the identified binding mode in cSrc to the kinase domain of EGFR supported that this interaction of the protonated tertiary amine of the inhibitor with the side chain of Asp348 in cSrc could be conserved in EGFR via the isostructural Asp800 and should result in increased potency when introduced into reversible inhibitors (Figure 3A). While all reversible quinolines showed a decreased affinity in drug resistant EGFR-Leu858Arg-Thr790Met, the irreversible inhibitors **3a** and **3b** retained potency in the subnanomolar range. These trends are well documented for 4-aminoquinazolines,[12] but to the best of our knowledge have not been reported for 4-aminoquinolines and can be directly linked to the enlarged amino acid side chain at the gatekeeper position.

Profiling the Cellular Activity of Quinolines. To determine the activity of the 4-anilinoquinolines in vitro, cellular-based screening of all the synthesized quinolines as well as on the structurally corresponding quinazolines and Erlotinib was performed in EGFR-dependent Ba/F3 cell lines. These cell lines express a series of clinically relevant EGFR-mutations, either with or without the Thr790Met gatekeeper mutation in EGFR (Figure 4a).[12] We found the quinolines to be active in all EGFR mutant Ba/F3 cells that

did not express the gatekeeper mutation, with GI_{50} values within the range of their structurally corresponding quinazolines. We next tested the ability of quinoline **3a** and **3e** to inhibit cell growth of patient derived NSCLC cell lines expressing mutant EGFR. Recapitulating our previous results, both quinolines robustly decreased viability of EGFR-mutated PC9 cells at submicromolar concentrations in the range of the activity of the quinazoline Erlotinib (Figure 4b). As expected, the irreversible quinoline **3a** is also active in cells (H1975) expressing the gatekeeper mutation Thr790Met in EGFR (Figure 4b). To assess the on-target activity of the quinolines, we determined the phosphorylation status of EGFR in PC9 cells after treatment with either **3a** or **3e** (Figure 4c), and this showed inhibition of EGFR autophosphorylation in a dose dependent manner.

Kinase Profiling. To compare the kinase inhibitor selectivity of our newly developed 4-anilinoquinolines with their quinazoline counterparts, kinase profiling was performed for **3e** and **3f** against a panel of 95 different protein kinases measuring the inhibition of kinase activity at a concentration of 10 μM (National Centre for Protein Kinase Profiling, University of Dundee, UK) (Figure 5). Both compounds showed the highest inhibitory effect, with equal potency, on the receptor tyrosine kinase HER4, the tyrosine kinases Lck and Yes1, as well as on the serine/threonine kinase RIPK2. Of particular interest was the finding that all these kinases possess a threonine at the gatekeeper position, suggesting that the N3 of the quinazoline inhibitor **3f** is unlikely to play a significant role in binding to these kinases. For the kinases that are weakly or moderately inhibited, a preference for one inhibitor over the other was observed. For example, the potency of the quinoline **3e** was higher than for the quinazoline counterpart **3f**, against EPBH-3, cSrc (Thr), and MINK1 (Met), while the quinazoline **3f** exhibited higher activity against PHK (Phe), PIM1 (Leu), and SmMLCK (Leu) kinases.

Conclusion

The improved understanding of kinase biology in disease states and a more precise description of inhibitor scaffold interactions with their target proteins has resulted in the design and development of a steadily increasing arsenal of potent and selective kinase inhibitors for targeted therapies and chemical biology research. Among the classical kinase inhibitors, compounds derived from ten-membered nitrogen-containing bicyclic scaffolds such as quinazolines represent a privileged chemotype that forms hydrogen bonds to the hinge region of the kinase domain and mimics the adenine ring of ATP. Several potent, quinoline-based type II inhibitors, which not only bind to the hinge region of the ATP pocket but also extend past the gatekeeper residue into an adjacent allosteric site to stabilize enzymatically inactive DFG-out kinase conformations, have been reported for p38α[20] and VEGFR,[21] respectively. However, quinoline-based type I inhibitors have been presumed to be suboptimal and are therefore clearly underrepresented in kinase inhibitor literature. In the present study, we demonstrate that reversible as well as irreversible inhibitors based on the 4-anilinoquinoline scaffold can be as potent as their quinazoline counterparts. In light of this observation, it is thus felt that they may serve as valuable starting points for further compound design.

Experimental Section

Chemistry. General. Unless otherwise noted, all reagents and solvents were purchased from Acros, Fluka, Sigma Aldrich, or Merck and used without further purification. ^{1}H and ^{13}C NMR spectra were recorded on a Bruker Avance DRX 400 spectrometer at 400 and 125 MHz or 100 MHz, respectively. Chemical shifts (δ) are given in ppm downfield from tetramethylsilane as an internal standard. Analytical TLC was carried out on Merck 60 F245 aluminum-backed silica gel plates. Compounds were purified by column chromatography using Baker silica gel (40−70 μm particle size). Preparative HPLC was conducted on a Varian HPLC system (Pro Star 215) with a VP 250/21 Nucleosil C18 PPN column from Macherey-Nagel and monitored by UV at 254 nm. High resolution electrospray ionization mass spectra (ESI-FTMS) were recorded on a Thermo LTQ Orbitrap (high resolution mass spectrometer from Thermo Electron) coupled to an "Accela" HPLC System supplied with a "Hypersil GOLD" column (Thermo Electron).

All tested compounds possessed a purity of >95% as determined by HPLC coupled with mass spectroscopy (HPLC-ESI-MS). HPLC-ESI-MS analyses were performed on an HPLC system from Agilent (1200 series) with an Eclipse XDB-C18, 5 μm (column dimensions: 150 mm × 4.60 mm) column from Agilent and UV detection at 254 nm coupled to a Thermo Finnigan LCQ Advantage Max ESI-spectrometer. H_2O with 0.1% formic acid (solvent A) and acetonitrile with 0.1% formic acid (solvent B) was used at a flow of 1 mL/min as a solvent system for HPLC-ESI-MS along with the gradient: 0 min, 90% solvent A/10% solvent B; 1 min, 90% solvent A/10% solvent B; 10 min, 0% solvent A/100% solvent B; 12 min, 0% solvent A/100% solvent B; 15 min, 90% solvent A/10% solvent B.

***N*-(4-(3-Bromophenylamino)quinolin-6-yl)acrylamide (3a).** Compound **3a** was prepared according to the literature procedure[12] using N^4-(3-bromophenyl)quinoline-4,6-diamine **11a** (0.32 g, 1.02 mmol), 250 mM solution of acryloyl chloride (4.07 mL, 1.02 mmol), *N*,*N*-diisopropylethylamine (266 μL, 1.5 mmol), and THF (103 mL) to produce the 62.0 mg (16.5%) of white solid after the preparative HPLC purification. ^{1}H NMR (400 MHz, DMSO-d_6) δ 10.85−10.42 (m, 2H), 9.07 (s, 1H), 8.50 (d, J = 6.8 Hz, 1H), 8.11−7.92 (m, 2H), 7.70 (s, 1H), 7.61−7.55 (m, 1H), 7.62−7.47 (m, 2H), 6.92 (d, J = 6.8 Hz, 1H), 6.53 (dd, J = 10.1, 17.0 Hz, 1H), 6.35 (dd, J = 1.9, 17.0 Hz, 1H), 5.86 (dd, J = 1.9, 10.1 Hz, 1H). ^{13}C NMR (125 MHz, DMSO) δ 164.47, 155.02, 142.95, 140.37, 138.52, 136.04, 132.59, 132.17, 130.59, 128.86, 128.62, 128.49, 124.82, 123.11, 122.36, 119.02, 112.59, 101.58. HRMS (ESI-MS) calcd 368.0393 for $C_{18}H_{15}BrN_3O$ [M + H$^+$], found 368.0397. LC-MS t_R = 6.7 min, purity ≥ 99%.

***N*-(4-(3-Bromophenylamino)quinolin-6-yl)propionamide (3c).** A 10 mL round-bottom flask was flushed with argon and charged with **11a** (0.1 g, 0.32 mmol), DIEPA (0.14 mL, 0.67 mmol), and dry THF and cooled down to 0 °C. Then a 100 mM solution of propionylchloride (0.28 mL, 0.32 mmol) was added dropwise to the reaction mixture. The reaction was stirred for an hour from 0 °C to room temperature. The progress of reaction was monitored by TLC, and upon completion the reaction mixture was basified with 10% aq $NaHCO_3$. The water phase was extracted with ethyl acetate (3 × 10 mL), and the combined organic layers were washed with water and dried over Na_2SO_4. The volatiles were removed in vacuo affording a yellow solid, which was further purified by column chromatography using DCM/MeOH (8:1) as an eluent to produce 42 mg (35%) of the title compound. ^{1}H NMR (400 MHz, DMSO-d_6) δ 10.17 (s, br, 1H), 9.02 (s, br, 1H), 8.62 (d, J = 2 Hz, 1H), 8.46 (d, J = 5.1 Hz, 1H), 7.86 (d, J = 9.0 Hz, 1H), 7.76 (dd, J = 2, 9.0 Hz, 1H), 7.50 (s, 1H), 7.38−7.28 (m, 2H), 7.22 (dd, J = 3.4, 5.4 Hz, 1H), 7.08 (d, J = 5.1 Hz, 1H), 2.40 (q, J = 7.5 Hz, 2H), 1.13 (t, J = 7.5, 3H). ^{13}C NMR (100 MHz, DMSO-d_6) δ 172.99, 149.76, 147.27, 146.43, 144.44, 137.01, 132.02, 130.24, 125.69, 124.50, 123.54, 122.95, 121.89, 119.85, 111.26, 105.15, 30.34, 10.53. HRMS

(ESI-MS) calcd 370.0550 for $C_{18}H_{17}BrN_3O$ [M + H$^+$], found: 370.0553. t_R = 6.5 min, purity = 98%.

***N*-(4-(3-Bromophenylamino)quinolin-6-yl)-4-(dimethylamino)-butanamide (3e).** (*E*)-4-(Dimethylamino)but-2-enoic acid hydrochloride (80 mg, 0.32 mmol) was stirred in 4 mL of THF under argon for 5 min. The solution was then cooled in an ice bath and DMF (50 μL) was added, followed by dropwise addition of oxalyl chloride (85 μL, 1.0 mmol). The reaction was stirred at room temperature for 2 h until a deep-orange color was observed. Then the reaction mixture was cooled in an ice bath for 10 min, and a solution of **11a** (0.1 g, 0.32 mmol) in 1-methyl-2-pyrrolidinone was added dropwise. Stirring was continued for the next 30 min in an ice bath, followed by stirring at room temperature for 2 h. Upon completion of the reaction, a saturated aqueous solution of $NaHCO_3$ was added to the reaction mixture until it became alkaline (pH 8−9). The resulting solid was then filtered off and purified by column chromatography (5−10% MeOH in DCM) to obtain a yellow solid product **3e** (56 mg, 41%); mp 186−187 °C. ^{1}H NMR (400 MHz, DMSO-d_6) δ 10.15 (s, 1H), 8.91 (s, 1H), 8.58 (s, 1H), 8.44 (d, J = 4.9 Hz, 1H), 7.83 (d, J = 9.0 Hz, 1H), 7.73 (dd, J = 2.2, 9.1 Hz, 1H), 7.47 (s, 1H), 7.33−7.26 (m, 3H), 7.18 (d, J = 6.9 Hz, 1H), 7.06 (d, J = 4.9 Hz, 1H), 2.38 (t, J = 7.3 Hz, 2H), 2.25 (t, J = 7.3 Hz, 2H), 2.13 (s, 6H), 1.74 (qn, J = 7.3 Hz, 2H). ^{13}C NMR (100 MHz, DMSO-d_6) δ 172.30, 147.16, 146.63, 144.35, 136.91, 132.04, 130.41, 125.73, 124.42, 123.56, 122.95, 121.85, 119.88, 111.18, 105.13, 59.27, 45.90, 34.98, 23.78. HRMS (ESI-MS) calcd 427.1128 for $C_{21}H_{24}BrN_4O$ [M + H$^+$], found 427.1126. t_R = 5.19 min, purity = 99.0%.

***N*-(3-Ethynylphenyl)-6,7-bis(2-methoxyethoxy)quinolin-4-amine (4a).** 3-Ethynylaniline 37.6 mg (0.32 mmol) and catalytic amount of 2N HCl (50 μL) was added to the solution of 4-chloro-6,7-bis(2-methoxyethoxy)quinoline (0.1 g, 0.32 mmol) in isopropyl alcohol, and reaction mixture was heated under reflux for 2 h. The reaction mixture was cooled to room temperature and basified with 10% aq sodium bicarbonate, followed by extraction with $CHCl_3$/MeOH (4:1). The combined organic layers were washed with water and dried over Na_2SO_4. The volatiles were removed in vacuo and resulting material was purified with column chromatography using CH_2Cl_2/MeOH (100:1 to 100:7) as an eluent to afford a 42 mg (33%) of yellow solid . ^{1}H NMR (400 MHz, CD_3CN) δ 9.52 (s, 1H), 8.06 (d, J = 6.8 Hz, 1H), 7.60 (s, 1H), 7.56−7.42 (m, 5H), 6.76 (d, J = 6.8 Hz, 1H), 4.31 (dd, J = 3.7, 5.3 Hz, 2H), 4.26−4.21 (m, 2H), 3.83−3.75 (m, 4H), 3.50 (s, 1H), 3.43 (s, 3H), 3.41 (s, 3H). ^{13}C NMR (100 MHz, CD3CN) δ 154.76, 153.21, 149.54, 139.92, 138.35, 136.04, 130.62, 130.56, 128.13, 125.73, 123.91, 112.40, 102.59, 101.28, 99.99, 82.63, 79.51, 70.57, 70.38, 69.15, 69.02, 58.64, 58.62. HRMS (ESI-MS) calcd 393.1809 for $C_{23}H_{25}N_2O_4$ [M + H$^+$], found 393.1812. t_R = 6.56 min, purity = 98.7%.

***N*-(3-Ethynylphenyl)-6,7-dimethoxyquinolin-4-amine (4b).** Compound **4b** was synthesized in the similar way as described for **4a** using 4-chloro-6,7-dimethoxyquinoline (0.2 g, 0.9 mmol), 3-ethynylaniline (0.1 g, 0.9 mmol), and catalytic amount of 2N HCl (50 μL). The crude was purified over silica gel using CH_2Cl_2/MeOH (100:1 to 100:5) as an eluent affording 0.24 g (86%) of **4b**; mp 253−255 °C. ^{1}H NMR (400 MHz, MeOD) δ 8.25 (d, J = 7.0 Hz, 1H), 7.88 (s, 1H), 7.60−7.48 (m, 4H), 7.30 (s, 1H), 6.86 (d, J = 7.0 Hz 1H), 4.10−4.00 (m, 6H), 3.68 (s, 1H). ^{13}C NMR (100 MHz, Me_3OD) δ 156.29, 154.32, 150.96, 139.61, 138.18, 136.05, 131.02, 130.41, 128.77, 126.02, 124.74, 112.39, 101.52, 99.66, 99.58, 82.19, 79.33, 56.08, 56.06. HRMS (ESI-MS) calcd 305.1285 for $C_{19}H_{17}N_3O_2$ [M + H$^+$], found 305.1284. t_R = 6.27 min, purity = 98.2%.

***N*-(3-Ethynylphenyl)-6,7-dimethoxyquinazolin-4-amine (4c).** Compound **4c** was synthesized by following the procedure described for **4a** using, 4,4-chloro-6,7-dimethoxyquinazoline (0.2 g, 0.9 mmol), 3-ethynylaniline (0.1 g, 0.9 mmol), and catalytic amount of 2N HCl (50 μL). The crude was purified over silica gel using CH_2Cl_2/MeOH (100:1 to 100:5) as an eluent affording 0.25 g (92%) of **4c**; mp 290−292 °C. ^{1}H NMR (400 MHz, MeOD) δ 8.73 (s, 1H), 7.99 (s, 1H), 7.88 (s, 1H), 7.74 (d, J = 7.8 Hz, 1H), 7.52−7.37 (m, 2H), 7.26 (s, 1H), 4.07 (s, 3H), 4.08 (s, 3H), 3.62 (s, 1H). ^{13}C NMR (100 MHz, MeOD) δ 159.06, 158.05, 151.85, 148.45, 137.34, 135.83, 130.15, 129.16, 127.82, 124.92, 123.48, 107.80, 102.74, 99.34, 82.59, 78.60, 56.34, 56.22. HRMS (ESI-MS) calcd 306.1237 for $C_{19}H_{16}N_3O_2$ [M + H$^+$], found 306.1236. t_R = 6.15 min, purity = 97.4%.

***N*-(4-(3-Bromophenylamino)quinazoline-6-yl)acrylamide (3b).** The compound is prepared according to the literature procedure[12] from N^4-(3-bromophenyl)-4,6-quinazolinediamine (0.3 g, 0.95 mmol), acryloyl chloride (95 μL, 1.14 mmol), *N*,*N*-diisopropylethylamine (380 mL, 2.29 mmol), and THF (103 mL) to produce 40 mg (11%) of white solid upon purification using preparative HPLC. ^{1}H NMR (400 MHz, DMSO-d_6): δ 10.48 (bs, 1H), 9.91 (bs, 1H), 8.82 (d, J = 2.2 Hz, 1H), 8.59 (s, 1H), 8.19 (t, J = 1.9 Hz, 1H), 7.93−7.85 (m, 2H), 7.79 (d, J = 9.0 Hz, 1H), 7.34 (t, J = 8.0 Hz, 1H), 7.31−7.26 (m, 1H), 6.53 (dd, J = 10.1, 17.0 Hz, 1H), 6.35 (dd, J = 1.9, 17.0 Hz, 1H), 5.83 (dd, J = 1.9, 10.1 Hz, 1H). ^{13}C NMR (100 MHz, DMSO-d_6): δ 163.34, 157.28, 153.18, 146.83, 141.14, 136.63, 131.54, 130.33, 128.56, 127.48, 127.24, 125.89, 124.24, 121.20, 120.77, 115.49, 112.24. HRMS (ESI-MS): calcd for $C_{17}H_{14}BrN_4O$ [M + H$^+$] 369.03455, found 369.03506. t_R = 7.12 min, purity = 99.4%.

***N*-(4-(3-Bromophenylamino)quinazoline-6-yl)propionamide (3d).** The compound was synthesized from N^4-(3-bromophenyl)-4,6-quinazolinediamine (0.1 g, 0.32 mmol), propionyl chloride (31 μL, 0.47 mmol), and *N*,*N*-diisopropylethylamine (110 μL, 0.67 mmol) in 3.5 mL of THF according to the literature.[22] An off-white solid (40 mg, 37%) was produced upon preparative HPLC. ^{1}H NMR (400 MHz, DMSO-d_6): δ 10.2 (s, 1H), 9.90 (s, 1H), 8.73 (s, 1H), 8.57 (s, 1H), 8.17 (s, 1H), 7.89−7.81 (m, 2H), 7.77 (d, J = 8.9 Hz, 1H), 7.34 (t, J = 8.0 Hz, 1H), 7.28 (d, J = 8.0 Hz, 1H), 2.41 (q, J = 7.5 Hz, 2H), 1.14 (t, J = 7.5 Hz, 3H). ^{13}C NMR (125 MHz, DMSO-d_6): δ 172.13, 157.22, 152.86, 146.46, 141.21, 137.05, 130.26, 128.36, 127.16, 125.77, 124.23, 121.09, 120.81, 115.45, 111.62, 29.36, 9.56. HRMS (ESI-MS): calcd for $C_{17}H_{16}{}^{79}BrN_4O$ [M + H$^+$] 371.05020, found 371.05074. t_R = 8.71 min, purity = 98.2%.

***N*-{4-[(3-Bromo-phenyl)amino]-quinazoline-6-yl}-4-(dimethyl-amino)butanamide (3f).** 4-(Dimethyl amino)-butyric acid hydrochloride (0.1 g, 0.506 mmol) and triethylamine (0.18 mL, 2.02 mmol) were stirred in 3 mL of DMF at 0 °C for 10 min. EDC·HCl (0.130 g, 1.01 mmol) was added, and the reaction mixture was further stirred for 10 min. The N^4-(3-bromophenyl)-4,6-quinazolinediamine (0.1 g, 0.31 mmol) was then added as a solid, and the reaction mixture was stirred at 0 °C for 30 min and then overnight at room temperature. On the next day, 0.5 mL of triethylamine was added, and the reaction mixture was extracted with ethyl acetate, washed with brine, and the organic phase was dried with sodium sulfate. Ethyl acetate was removed to obtain an oily residue which was purified by preparative HPLC to obtain 27 mg (19%) of a pale-yellow solid. ^{1}H NMR (400 MHz, DMSO-d_6): δ 10.25 (s, 1H), 9.88 (s, 1H), 8.72 (d, J = 1.9 Hz, 1H), 8.57 (s, 1H), 8.16 (t, J = 1.9 Hz, 1H), 7.89−7.81 (m, 2H), 7.75 (d, J = 8.9 Hz, 1H), 7.34 (t, J = 8.0 Hz, 1H), 7.30−7.26 (m, 1H), 2.42 (t, J = 7.4 Hz, 2H), 2.27 (t, J = 7.1 Hz, 2H), 2.15 (s, 6H), 1.77 (qn, J = 7.2 Hz, 2H). ^{13}C NMR (125 MHz, DMSO-d_6): δ 171.36, 157.23, 152.86, 146.48, 141.21, 137.05, 130.25, 128.37, 127.13, 125.77, 124.25, 121.07, 120.83, 115.45, 111.53, 58.46, 45.11(2 × C), 34.02, 22.92. HRMS (ESI-MS): calcd for $C_{20}H_{23}BrN_5O$ [M + H$^+$] 428.10805, found 428.10792. t_R = 6.18 min, purity = 98.3%.

Kinetics Assay for IC_{50} Determination. IC_{50} determinations for wild type and mutants of EGFR were measured with the HTRF KinEASE-TK assay from Cisbio according to the manufacturer's instructions. A biotinylated poly Glu-Tyr substrate peptide was phosphorylated by EGFR. After completion of the reaction, an antiphosphotyrosine antibody labeled with europium cryptate and streptavidin labeled with the fluorophore XL665 were added. The FRET between europium cryptate and XL665 was measured to quantify the phosphorylation of the

substrate peptide. ATP concentrations were set at their respective K_m values (30 μM for the EGFR-WT, 60 μM for EGFR-Leu858Arg, and 30 μM for EGFR-Leu858Arg, Thr790Met), and 50 nM of substrate were used for both wild type and mutant EGFR. Kinase, substrate peptide, and inhibitor were preincubated for 2 h before the reaction was started by addition of ATP. A Tecan Safire^2 plate reader was used to measure the fluorescence of the samples at 620 nm (Eu-labeled antibody) and 665 nm (XL665 labeled streptavidin) 60 μs after excitation at 317 nm. The quotient of both intensities for reactions made with eight different inhibitor concentrations (including no inhibitor) were plotted against inhibitor concentrations and fit to a Hill 4-parameter equation to determine IC_{50} values. Each reaction was performed in duplicate, and at least three independent determinations of each IC_{50} were made.

Structural Modeling. The small molecule structures of 4-anilinoquinolines were sketched and minimized in DS ViewerPro (http://www.accelrys.com) and aligned to the kinase domains of the EGFR-erlotinib (PDB code: 1M17) and EGFR−**3b** complexes (PDB code: 2J5F) using PyMol (http://www.pymol.org). In the modeled 4-anilinoquinoline EGFR complexes, the inhibitors adopt binding modes isostructural to erlotinib or **3b** in EGFR. N1 of the quinoline scaffold forms one key hydrogen bond to the backbone of the hinge region (Met793 in EGFR).

Cell Lines. NSCLC cells were obtained from ATCC (www.atcc.org) and were maintained as described previously.[23] Ba/F3 cell lines were established as described previously[24] and were maintained in RPMI media containing 10% FCS and 1% of penicillin and streptomycin.

Viability Assays. The assay was set out as described previously.[25] In brief, cells were plated into sterile 96-well plates using a Multidrop instrument (www.thermo.com) and after 24 h of incubation a dilution series of compounds was added. Viability was determined after 96 h using the Cell Titer-Glo assay (www.promega.com). Luminescence was measured on a Mithras LB940 plate reader (www.bertholdtech.com). Half-maximal inhibitory concentrations were determined using the R package "ic50".

Immunoblotting. Immunoblotting was performed using standard procedures as described before.[25] Briefly, cells were treated for 24 h and concentration of a given compound prior to using whole cell lysates for immunoblotting. The following antibodies were utilized: p-EGFR (Biosource, USA), antirabbit-antibody, antimouse (Millipore, Germany). The enhanced chemiluminescence (ECL) system (Amersham-Pharmacia) was used to develop the blots.

Acknowledgment. We thank Rogier Buijsman and Michael Beck for helpful discussions. The work was supported by the German Federal Ministry for Education and Research through the German National Genome Research Network-Plus (NGFN-Plus) (BMBF grant 01GS08102), all to D.R., and by the Deutsche Krebshilfe (grant 107954), by the Fritz-Thyssen-Stiftung (grant 10.08.2.175) as well as by the German National Genome Research Network-Plus (NGFN-Plus) (BMBF grant 01GS08100), all to R.K.T. W.A.L.vO. thanks the Alexander von Humboldt Foundation for a Georg Forster Research Fellowship for Experienced Researchers and the University of the Witwatersrand for sabbatical leave. Schering Plough, Bayer-Schering Pharma, Merck-Serono, and Bayer CropScience are thanked for financial support.

Supporting Information Available: Figure and experimental data for compounds **7**, **8a**, **11a**, **15a**. This material is available free of charge via the Internet at http://pubs.acs.org.

References

(1) Sharma, S. V.; Bell, D. W.; Settleman, J.; Haber, D. A. Epidermal growth factor receptor mutations in lung cancer. *Nat. Rev. Cancer* **2007**, *7*, 169–181.

(2) Backes, A. C.; Zech, B.; Felber, B.; Klebl, B.; Müller, G. Small-molecule inhibitors binding to protein kinases. Part I: exceptions from the traditional pharmacophore approach of type I inhibition. *Expert Opin. Drug Discovery* **2008**, *3*, 1409–1425.

(3) Backes, A. C.; Zech, B.; Felber, B.; Klebl, B.; Müller, G. Small-molecule inhibitors binding to protein kinase. Part II: the novel pharmacophore approach of type II and type III inhibition. *Expert Opin. Drug Discovery* **2008**, *3*, 1427–1449.

(4) Pao, W.; Miller, V.; Zakowski, M.; Doherty, J.; Politi, K.; Sarkaria, I.; Singh, B.; Heelan, R.; Rusch, V.; Fulton, L.; Mardis, E.; Kupfer, D.; Wilson, R.; Kris, M.; Varmus, H. EGF receptor gene mutations are common in lung cancers from "never smokers" and are associated with sensitivity of tumors to gefitinib and erlotinib. *Proc. Natl. Acad. Sci. U.S.A.* **2004**, *101*, 13306–13311.

(5) Rewcastle, G. W.; Denny, W. A.; Bridges, A. J.; Zhou, H. R.; Cody, D. R.; McMichael, A.; Fry, D. W. Tyrosine kinase inhibitors. 5. Synthesis and structure−activity relationships for 4-[(phenylmethyl)amino]- and 4-(phenylamino)quinazolines as potent adenosine 5′-triphosphate binding site inhibitors of the tyrosine kinase domain of the epidermal growth factor receptor. *J. Med. Chem.* **1995**, *38*, 3482–3487.

(6) Wissner, A.; Berger, D. M.; Boschelli, D. H.; Floyd, M. B.; Greenberger, L. M.; Gruber, B. C.; Johnson, B. D.; Mamuya, N.; Nilakantan, R.; Reich, M. F.; Shen, R.; Tsou, H. R.; Upeslacis, E.; Wang, Y. F.; Wu, B. Q.; Ye, F.; Zhang, N. 4-Anilino-6,7-dialkoxyquinolime-3-carbonitrile inhibitors of epidermal growth factor receptor kinase and their bioisosteric relationship to the 4-anilino-6,7-dialkoxyquinazoline inhibitors. *J. Med. Chem.* **2000**, *43*, 3244–3256.

(7) Wissner, A.; Mansour, T. S. The development of HKI-272 and related compounds for the treatment of cancer. *Arch. Pharm.* **2008**, *341*, 465–477.

(8) Stamos, J.; Sliwkowski, M. X.; Eigenbrot, C. Structure of the epidermal growth factor receptor kinase domain alone and in complex with a 4-anilinoquinazoline inhibitor. *J. Biol. Chem.* **2002**, *277*, 46265–46272.

(9) Hennequin, L. F.; Allen, J.; Breed, J.; Curwen, J.; Fennell, M.; Green, T. P.; Lambert-van der Brempt, C.; Morgentin, R.; Norman, R. A.; Olivier, A.; Otterbein, L.; Ple, P. A.; Warin, N.; Costello, G. *N*-(5-Chloro-1,3-benzodioxol-4-yl)-7-[2-(4-methylpiperazin-1-yl)ethoxy]-5- (tetrahydro-2*H*-pyran-4-yloxy)quinazolin-4-amine, a novel, highly selective, orally available, dual-specific c-Src/Abl kinase inhibitor. *J. Med. Chem.* **2006**, *49*, 6465–6488.

(10) Rachid, Z.; Brahimi, F.; Qiu, Q.; Williams, C.; Hartley, J. M.; Hartley, J. A.; Jean-Claude, B. J. Novel nitrogen mustard-armed combi-molecules for the selective targeting of epidermal growth factor receptor overexperessing solid tumors: Discovery of an unusual structure−activity relationship. *J. Med. Chem.* **2007**, *50*, 2605–2608.

(11) Wissner, A.; Fraser, H. L.; Ingalls, C. L.; Dushin, R. G.; Floyd, M. B.; Cheung, K.; Nittoli, T.; Ravi, M. R.; Tan, X. Z.; Loganzo, F. Dual irreversible kinase inhibitors: quinazoline-based inhibitors incorporating two independent reactive centers with each targeting different cysteine residues in the kinase domains of EGFR and VEGFR-2. *Bioorg. Med. Chem.* **2007**, *15*, 3635–3648.

(12) Michalczyk, A.; Klüter, S.; Rode, H. B.; Simard, J. R.; Grütter, C.; Rabiller, M.; Rauh, D. Structural insights into how irreversible inhibitors can overcome drug resistance in EGFR. *Bioorg. Med. Chem.* **2008**, *16*, 3482–3488.

(13) Carter, T. A.; Wodicka, L. M.; Shah, N. P.; Velasco, A. M.; Fabian, M. A.; Treiber, D. K.; Milanov, Z. V.; Atteridge, C. E.; Biggs, W. H., 3rd; Edeen, P. T.; Floyd, M.; Ford, J. M.; Grotzfeld, R. M.; Herrgard, S.; Insko, D. E.; Mehta, S. A.; Patel, H. K.; Pao, W.; Sawyers, C. L.; Varmus, H.; Zarrinkar, P. P.; Lockhart, D. J. Inhibition of drug-resistant mutants of ABL, KIT, and EGF receptor kinases. *Proc. Natl. Acad. Sci. U.S.A* **2005**, *102*, 11011–11016.

(14) Pao, W.; Miller, V. A.; Politi, K. A.; Riely, G. J.; Somwar, R.; Zakowski, M. F.; Kris, M. G.; Varmus, H. Acquired resistance of lung adenocarcinomas to gefitinib or erlotinib is associated with a second mutation in the EGFR kinase domain. *PLoS Med.* **2005**, *2*, 225–235.

(15) Yun, C. H.; Mengwasser, K. E.; Toms, A. V.; Woo, M. S.; Greulich, H.; Wong, K. K.; Meyerson, M.; Eck, M. J. The T790M mutation in EGFR kinase causes drug resistance by increasing the affinity for ATP. *Proc. Natl. Acad. Sci. U.S.A* **2008**, *105*, 2070–2075.

(16) Getlik, M.; Grütter, C.; Simard, J. R.; Klüter, S.; Rabiller, M.; Rode, H. B.; Robubi, A.; Rauh, D. Hybrid compound design to overcome the gatekeeper T338M mutation in cSrc. *J. Med. Chem.* **2009**, *52*, 3915–3926.

(17) Sos, M. L.; Rode, H. B.; Heynck, S.; Peifer, M.; Fischer, F.; Klüter, S.; Pawar, V.; Reuter, C.; Heuckmann, J. M.; Weiss, J.; Ruddigkeit,

L.; Rabiller, M.; Koker, M.; Simard, J. R.; Getlik, M.; Yuza, Y.; Chen, J. Y.; Greulich, H.; Thomas, R. K.; Rauh, D. Insights into the limited activity of irreversible EGFR inhibitors in tumor cells expressing the T790M EGFR resistance mutation from chemogenomics profiling. *Cancer Res.* **2010**, *70*, 859–862.

(18) Hennequin, L. F.; Thomas, A. P.; Johnstone, C.; Stokes, E. S. E.; Ple, P. A.; Lohmann, J. J. M.; Ogilvie, D. J.; Dukes, M.; Wedge, S. R.; Curwen, J. O.; Kendrew, J.; Lambert-van der Brempt, C. Design and structure−activity relationship of a new class of potent VEGF receptor tyrosine kinase inhibitors. *J. Med. Chem.* **1999**, *42*, 5369–5389.

(19) Furuta, T.; Sakai, T.; Senga, T.; Osawa, T.; Kubo, K.; Shimizu, T.; Suzuki, R.; Yoshino, T.; Endo, M.; Miwa, A. Identification of potent and selective inhibitors of PDGF receptor autophosphorylation. *J. Med. Chem.* **2006**, *49*, 2186–2192.

(20) Klüter, S.; Grütter, C.; Naquvi, T.; Rabiller, M.; Simard, J. R.; Pawar, V.; Getlik, M.; Rauh, D. Design of a displacement assay for kinases based on a DFG-out binding probe. *J. Med. Chem.* **2009**, *53*, 357–367.

(21) Harmange, J.-C.; Weiss, M. M.; Germain, J.; Polverino, A. J.; Borg, G.; Bready, J.; Chen, D.; Choquette, D.; Coxon, A.; DeMelfi, T.; DiPietro, L.; Doerr, N.; Estrada, J.; Flynn, J.; Graceffa, R. F.; Harriman, S. P.; Kaufman, S.; La, D. S.; Long, A.; Martin, M. W.; Neervannan, S.; Patel, V. F.; Potashman, M.; Regal, K.; Roveto, P. M.; Schrag, M. L.; Starnes, C.; Tasker, A.; Teffera, Y.; Wang, L.; White, R. D.; Whittington, D. A.; Zanon, R. Naphthamides as Novel and Potent Vascular Endothelial Growth Factor Receptor Tyrosine Kinase Inhibitors: Design, Synthesis, and Evaluation. *J. Med. Chem.* **2008**, *51*, 1649–1667.

(22) Bridges, A. J.; Denny, W. A.; Dobrusin, E. M.; Doherty, A. M.; Fry, D. W.; McNamara, D. J.; Showalter, H. D. H.; Smaill, J. B.; Zhou, H. et al. et al. Preparation of *N*-quinazolinylacrylamides and analogs as tyrosine kinase inhibitors. U.S. Patent 97-US5778 9738983, 19970408, 1997.

(23) Sos, M. L.; Michel, K.; Zander, T.; Weiss, J.; Frommolt, P.; Peifer, M.; Li, D.; Ullrich, R.; Koker, M.; Fischer, F.; Shimamura, T.; Rauh, D.; Mermel, C.; Fischer, S.; Stuckrath, I.; Heynck, S.; Beroukhim, R.; Lin, W.; Winckler, W.; Shah, K.; LaFramboise, T.; Moriarty, W. F.; Hanna, M.; Tolosi, L.; Rahnenfuhrer, J.; Verhaak, R.; Chiang, D.; Getz, G.; Hellmich, M.; Wolf, J.; Girard, L.; Peyton, M.; Weir, B. A.; Chen, T. H.; Greulich, H.; Barretina, J.; Shapiro, G. I.; Garraway, L. A.; Gazdar, A. F.; Minna, J. D.; Meyerson, M.; Wong, K. K.; Thomas, R. K. Predicting drug susceptibility of non-small cell lung cancers based on genetic lesions. *J. Clin. Invest.* **2009**, *119*, 1727–1740.

(24) Yuza, Y.; Glatt, K. A.; Jiang, J. R.; Greulich, H.; Minami, Y.; Woo, M. S.; Shimamura, T.; Shapiro, G.; Lee, J. C.; Ji, H. B.; Feng, W.; Chen, T. H.; Yanagisawa, H.; Wong, K. K.; Meyerson, M. Allele-dependent variation in the relative cellular potency of distinct EGFR inhibitors. *Cancer Biol. Ther.* **2007**, *6*, 661–667.

(25) Sos, M. L.; Koker, M.; Weir, B. A.; Heynck, S.; Rabinovsky, R.; Zander, T.; Seeger, J. M.; Weiss, J.; Fischer, F.; Frommolt, P.; Michel, K.; Peifer, M.; Mermel, C.; Girard, L.; Peyton, M.; Gazdar, A. F.; Minna, J. D.; Garraway, L. A.; Kashkar, H.; Pao, W.; Meyerson, M.; Thomas, R. K. PTEN Loss Contributes to Erlotinib Resistance in EGFR-Mutant Lung Cancer by Activation of Akt and EGFR. *Cancer Res.* **2009**, *69*, 3256–3261.

(26) Blair, J. A.; Rauh, D.; Kung, C.; Yun, C. H.; Fan, Q. W.; Rode, H.; Zhang, C.; Eck, M. J.; Weiss, W. A.; Shokat, K. M. Structure-guided development of affinity probes for tyrosine kinases using chemical genetics. *Nat. Chem. Biol.* **2007**, *3*, 229–238.